Role of Pouring Parameters on Mechanical Properties of Aluminum Alloys

Scott R. Giese
Justine Radunzel
University of Northern Iowa, Cedar Falls, Iowa, USA

Maria Alverio-Kapka
Carley Foundry, Blaine, Minnesota, USA

ABSTRACT

Aluminum alloys are notorious for forming an oxide film during gravity filling, potentially becoming incorporated into the molten metal from turbulence. This research objective explored if pouring parameters of temperature and pouring height influence mechanical properties of aluminum alloys due to the oxide film. An experimental design considered these parameters for A356 and A206 alloys. Replicated castings were poured at a foundry using temperatures of 732C (1350F) and 774C (1425F) at pouring heights of 12 cm (4.72 in.) and 24 cm (9.45 in.), respectively. A linear mixed model analysis of variance technique was used to determine if there was an effect on strength properties and ductility. Pouring temperature was determined to be significant on mechanical properties, though only with certain properties depending on the alloy. The main factor of pouring height showed no significant effect on mechanical properties. Alloy chemistry was postulated to have a contribution on oxide formation with respect to mechanical properties.

Keywords: aluminum alloys, pouring height, pouring temperature, air entrainment, oxide inclusions

INTRODUCTION

The University of Northern Iowa was awarded a contract from the Defense Logistics Agency (DLA), contract numbers SP4701-18-D-1200 and SP4701-18-F-0070, titled “Investigation of Dross Mechanism for Highly Oxidative Casting Alloys.” The main research objective of the five-year project was to understand the complex nature of dross formation in highly oxidative type alloys, such as aluminum. It is widely accepted in the aluminum foundry industry that the performance of these alloys is strongly affected by air entrainment and dross formation on exposed surfaces of liquid aluminum. Simulation tools have satisfactorily addressed predicting air entrainment and oxide formation but use empirical relationships, assumptions, and two-phase analogous observations.[1-3] The research project addressed these technical gaps for air entrainment and oxide formation to improve computational tools for future machine learning and digital twin applications.

One area pursued in the research work was air entrainment, mainly because of the complexity of the threshold for air entrainment, especially in metalcasting situations. A transparent water apparatus, coupled with high-speed videography, was designed to focus on the transitional area of air entrainment between laminar conditions producing no bubbles to strong disturbances causing cratering (gross bubble formation) and liquid disassociation. From the research work, it was found that air entrainment is more than just a direct conversion of jet disturbances into bubble volume, but a complex and disordered balance between surface disturbances, micro-turbulent jet flow, and the restoring force of surface tension.[4]

Oxide formation is a multifaceted reaction to form simple and complex oxides based on the alloy chemical composition at a given temperature. Figure 1 shows an Ellingham diagram of pure metals and the equilibrium balance of oxidative type environments. Though the research work could not develop a thermodynamic interaction database because of the high oxygen affinity of the aluminum solute prior to liquification for nickel aluminum bronze, low aluminum solute addition in copper did demonstrate that temperature strongly affects the kinetics for oxygen dissolution.

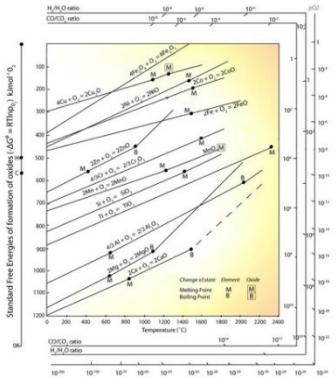

Figure 1. Ellingham diagram of selected metallic oxide systems from the University of Cambridge.[5]

Figure 2 shows images obtained from high speed videography captured at 1000 fps of molten A356 aluminum exiting a 10 mm hole captured the DLA research work. In Figure 2(a), thin bands of oxide film form and separate at the exit point. These bands help develop perturbation harmonics that cause the molten stream to elongate and distort as the liquid aluminum accelerates. The oxide film, as observed toward the end of pouring, appears to be buckling and containing the volume of metal. When the pouring temperature is lowered, the oxide film has a thin, sheet film appearance and the perturbation frequency is higher. It was surmised that temperature has a critical role on the perturbation harmonics, which in turn, as discussed by Relph and Kiger,[4] changes the incipient pool characteristics and interactions in generating air bubbles.

(a) (b)

Figure 2. Still frame captures of molten A356 aluminum stream. (a) A356 aluminum poured at 1600F (871C) with the left photo during steady state conditions and the right photo captured toward the end of pouring. Thin oxide bands formed but defined harmonics were observed, and fluid motion is distorted from oxide film buckling. (b) A356 aluminum poured at 1250F (675C) with the left photo during steady state conditions and the right photo captured toward the end of pouring. Longer oxide bands were observed though irregular harmonics were developed from the variable length of the oxide film developed after separation.

DESIGN OF EXPERIMENTS

Casting trials were developed using a similar casting design used in Runyoro, Boutorati, and Campbell investigation of the role of inclusions on performance of A356 aluminum.[6] The experimental approach was modified to test two factors observed in high-speed videography shown in Figure 2. The first hypothesis factor considered was based on the common assumption that higher pouring temperatures will cause more oxidation products. The second hypothesis factor considered was pouring height distance produces more surface area for oxidization exposure.

The experimental casting was to develop as a representative sample of cylinders that could be easily machined into ½ in (1.27 cm) ASTM E8 tensile bars. The Runyoro, Boutorati, and Campbell design[6] was modified to statistically test the two hypothesis factors without other oxide formation potentials. To overcome oxide formation issues such as dynamic fluid jumps and turbulence during gating system priming, the design incorporated a large overflow reservoir to remove surface oxides formed during initial casting filling. The overall casting design configuration was approximately 35 lbs. in design weight to capture oxide films generated by the pouring stream steady state flow conditions from the ladle to the pouring cup and minimize oxide film formation from initial transient filling, casting cavity turbulence, and pouring cup influences.

EXPERIMENTAL METHODOLOGY

A pattern was designed to bottom fill eight cylinders similar to the casting design shown in Figure 3, to be turned into standard ASTM E8 0.505 in. (1.283 cm) tensile bars. The casting gating system was modified and designed using Flow Science Flow 3D® CFD software to observe the filling pattern for an unfiltered gating system and accommodate the larger size casting. A total of sixteen vertically-parted molds were produced using 0.7% commercially available phenolic urethane binder system, and a blend of ~30% thermal and ~70% mechanical reclaimed silica sand.

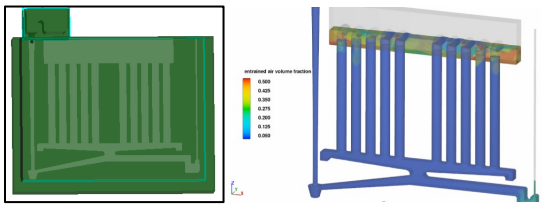

Figure 3. Casting design used to produce 8-½ in (1.27 cm ASTM E8 tensile bars per pour. The simulation view on the right shows the overflow reservoir minimized air entrainment during steady state pouring conditions.

Two electric furnaces were used for the experiment, one 2,300 lb. furnace was filled with A365, and another identical size furnace was filled with A206. Preparation of the molten A2065 and A356 aluminum used standard foundry practices at the participating aluminum foundry, respectively. Prior to pouring castings, the furnace was degassed with an argon sparging gas, and the alloys were degassed to a specific gravity of 2.62 and 2.75 respectively for A356 and A206. A total of eight molds were poured for each alloy. Two replicates were cast at each temperature and height from the pouring cup. See

Tables 1 and 2, for the full factorial statistically designed experiment using the parameters of pouring temperature and pouring height.

Table 1. A356 Full Factorial Experimental Design

	TEMPERATURE (°C)	POURING HEIGHT (cm)
LOW	732	12
HIGH	774	24

Table 2. A206 Full Factorial Experimental Design

	TEMPERATURE (°C)	POURING HEIGHT (cm)
LOW	732	12
HIGH	774	24

The molds were set up under a stand that would hold the two-man #30 graphite crucible secured in a ladle shank at one of the two desired heights for the duration of pouring. The pouring height presented in the experimental design was measured from the bar of the ladle holder to the predetermined pool height in the pouring cup. Though the true pouring distance from the crucible lip to molten aluminum pool height in the pouring cup will change during pouring, rotation and maintenance of the height remained constant.

The #30 crucible was preheated until it was orange in color and then filled with aluminum and a 5% titanium 1% boron additive for grain refinement. No strontium treatment was performed. When the two-man ladle was resting on the stand and the hand-held thermocouple read the desired temperature, the pourer poured as fast as possible to keep the pouring cup and sprue full during filling. As the ladle was turned, the molten metal was released from the cup from a higher point transitioning to a lower point as the ladle emptied. The handle rested on the bar for the duration of the pour to keep each mold as consistent as possible.

The castings were sectioned into eight cylinders, and heat treated in a cycle according to the alloy specifications. The A356 was solutioned at 1000F (538C) for 12 hours, quenched in a water bath held between 150-180F (66-82C), followed by an aging treatment at 310F (154C) for five hours. The A206 had a stepwise solution treatment of 910F (488C) for two hours, 950F (510C) for two hours, and 985F (529C) for twelve hours followed by a water quench between 150-180F (66-82C). No aging treatment was performed on the A206 cylinders. The cylinders were turned into ASTM E8 0.505 in. (1.283 cm) tensile bars on a lathe and pulled for mechanical properties.

STATISTICAL ANALYSIS

A linear mixed model (LMM) was estimated for the tensile strength, yield strength, and elongation outcomes. The LMM included main factor of temperature (1350 F (732C) vs. 1425 F (774C)), pouring height (lower representing 12 cm (4.72 in.) vs. higher representing 24 cm (9.45 in.)), and a temperature x pouring height interaction for the fixed effects. The model accounted for the repeated measures due to there being multiple bars being measured from the same casting. The Bayesian Information Criterion (BIC) was used to select the appropriate covariance structure from among first-order autoregressive structure with homogeneous variances (AR(1)), first-order autoregressive structure with heterogenous variances (ARH(1)), compound symmetry (CS), heterogenous compound symmetry (CSH), Toeplitz (TP), and Toeplitz heterogenous (TPH).[7] A lower BIC value indicates a better fitting model. A Satterthwaite adjustment was used to compute the degrees of freedom with a significance level of 0.05 used in the study. The assumption of the outcome variables following a normal distribution seemed reasonably satisfied based on histograms and normal QQ-plots that are not presented in the paper. Analyses were conducted separately by alloy (A206 vs. A356). The statistical package SPSS 29.0 was used for the analyses.

PRESENTATION OF RESULTS

Notation for the presentation of the statistical analysis was (F(Ndf, Ddf) = F, p = #) where Ndf is the Numerator degrees of freedom, Ddf is the Denominator, F is the F statistic value, and p is the significance value for the F statistics. In the presentation of results, CI represents Confidence Interval.

LMM RESULTS FOR TENSILE STRENGTH

A206

The BIC for AR(1) covariance structure = 1,193.61 for the statistical analysis of A206 tensile strength. The constant variance for the AR(1) covariance structure was estimated to be 23,433,842.95 (Wald Z = 4.21, p < .001), and the ρ (the correlation between adjacent bars) was estimated to be 0.43 (Wald Z = 3.05, p = .002). The LMM results for A206 tensile strength showed no significant interaction between temperature and pouring height ($F(1,10.22) = 1.74$, $p = .216$). Additionally, there was neither a significant temperature main effect ($F(1,10.22)=0.39$, $p = .548$) or significant pouring height main effect ($F(1,10.22)=0.25$, $p = .631$).

Table 3 provides the marginal means for tensile strength estimated from LMM by temperature and pouring height for alloy A206, and Figure 4 provides the LMM marginal means for tensile strength and the corresponding 95% confidence intervals by temperature and pouring height. The difference between the lower bound and upper bound confidence interval was approximately 7,800 psi for all

experimental conditions presented in Table 3. For lower temperature, lower pouring height exhibited the highest mean tensile strength. When a higher temperature was considered, higher pouring height displayed a slightly higher mean tensile strength.

Table 3. Means and Confidence Intervals for Tensile Strength of A206 by Temperature (Temp) and Pouring Height (Height)

			95% Confidence Interval	
Temp	Height	Mean (psi)	Lower Bound	Upper Bound
1350	Lower	54,102	50,212	57,991
	Higher	50,923	47,033	54,812
1425	Lower	50,702	46,812	54,592
	Higher	52,146	48,257	56,035

Standard Error = 1750.77
All units for Means and Confidence Interval are psi.

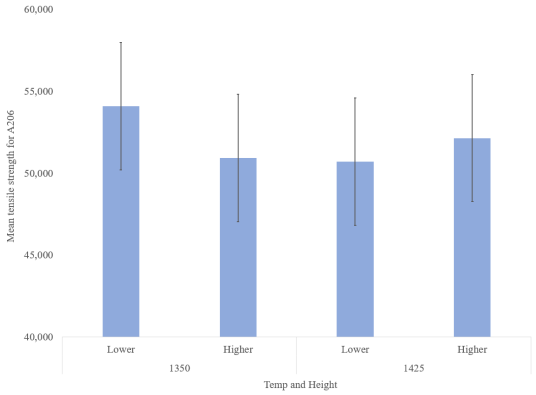

Figure 4. The LMM marginal means for tensile strength A206 (and 95% confidence intervals) by temperature (temp) and pouring height (height).

A356

Statistical analysis for A356 produced a BIC value for AR(1) covariance structure = 1034.58. The constant variance for the AR(1) covariance structure was estimated to be 1,308,648.13 (Wald Z = 5.45, p < 0.001), and the ρ (the correlation between adjacent bars) was estimated to be 0.01 (Wald Z = 0.04, p = 0.966). The LMM results identified a significant interaction between temperature and pouring height on tensile strength for A356 ($F(1, 20.52) = 5.47$, $p = 0.030$). Statistical analysis of the main effect yielded no significance with temperature ($F(1, 20.52) = 1.74$, $p = 0.202$) or significance on pouring ($F(1, 20.52) = 0.11$, $p = 0.748$) for A356 tensile properties.

Table 4 provides the marginal means for tensile strength estimated from LMM by temperature and pouring height for alloy A356, and Figure 5 provides the LMM marginal means for tensile strength and the corresponding 95% confidence intervals by temperature and pouring height.

The difference between the lower bound and upper bound confidence interval was approximately 1,200 psi (8.27 MPa) for all experimental conditions presented in Table 4. Like A206, the lower pouring height exhibited the higher mean tensile strength. For higher pouring temperature, higher pouring height displayed a slightly higher mean tensile strength of approximately 800 psi (5.52 MPa).

Table 4. Means and Confidence Intervals for Tensile Strength of A356 by Temperature (Temp) and Pouring Height (Height)

			95% Confidence Interval	
Temp	Height	Mean (psi)	Lower Bound	Upper Bound
1350	Lower	34,226	33,628	34,825
	Higher	33,648	33,049	34,247
1425	Lower	33,176	32,577	33,744
	Higher	33,941	33,343	34,540

Standard Error = 287.45
All units for Means and Confidence Interval are psi.

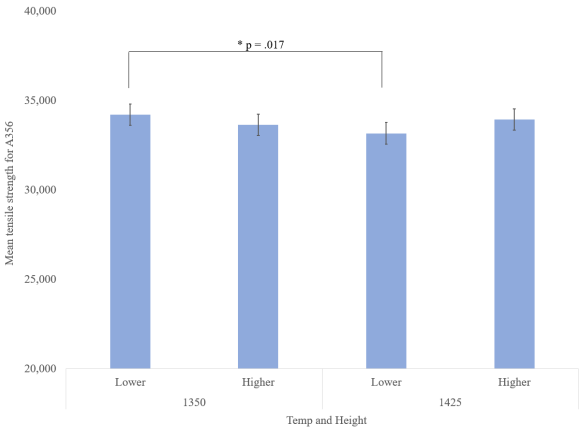

Figure 5. The LMM marginal means for tensile strength A356 (and 95% confidence intervals) by temperature (temp) and pouring height (height).

Because of the interaction significance indication of the LMM analysis for A356, a factor isolation analysis was performed to understand the contributing factor to the interaction significance. The standard error for the analysis was 406.52. For lower pouring height, there was a significant difference in the mean tensile strength for A356 between 1350F (732C) and 1425F (774C) ($p = .017$, mean difference = 1,051 psi (7.24 MPa), 95% CI for mean difference = 204 psi (1.41 MPa) to 1,897 psi (13.08 MPa).

On the other hand, for higher pouring height, there was no significant difference in the mean tensile strength for A356 between 1350F (732C) and 1425F (774C) ($p = .479$, mean difference = -293 psi (-2.02 MPa), 95% CI of

mean difference = -1,140.05 to 553 psi (-7.86 to 3.81 MPa). A pouring height comparison for tensile strength A356 within temperature yielded no significant difference in the mean tensile strength for A356 between the lower and higher height groups (p = .170 for 1350F (732C) and p = .074 for 1425F (774C)). Therefore, the comparison statistical analysis indicates the interaction significance is attributable to lower pouring height for pouring temperatures between 1350F (732C) and 1425F (774C).

LMM RESULTS FOR YIELD STRENGTH

A206

An LMM statistical analysis was performed for A206 yield strength considering pouring temperature and pouring height. BIC for ARH(1) covariance structure equaled 1043.02 for the A206 yield strength analysis. The variance for the ARH(1) covariance structure varied across the bars from 25,364.50 for bar 1 (Wald Z = 1.16, p = .246) to 8,424,278.73 for bar 6 (Wald Z = 2.33, p = .020), and the ρ (the correlation between adjacent bars) was estimated to be 0.72 (Wald Z = 6.98, p < .001). The LMM analysis indicated a significant interaction between pouring temperature and pouring height on yield strength for A206 (F(1, 3.55)=22.16, p = .012). Statistical analysis of the main effect identified significance with temperature (F(1, 3.55) = 192.24, p = <0.001). No significant effect of pouring height (F(1, 3.55) = 6.26, p = 0.074) was determined for A206 yield strength properties.

Table 5 provides the marginal means for A206 yield strength estimated from LMM by temperature and pouring height, and Figure 6 provides the LMM marginal means for tensile strength and the corresponding 95% confidence intervals by temperature and pouring height. The difference between the lower bound and upper bound confidence interval was approximately 475 psi for all experimental conditions presented in Table 5. For lower temperature, lower pouring height exhibited the higher mean tensile strength, but the difference was only 148 psi. When higher temperature was considered, higher pouring height displayed a higher mean tensile strength and overall yield strength difference compared to lower pouring temperature was observable less for both pouring height.

Table 5. Means and Confidence Intervals for Yield Strength of A206 by Temperature (Temp) and Pouring Height (Height)

			95% Confidence Interval	
Temp	Height	Mean (psi)	Lower Bound	Upper Bound
1350	Lower	39,330	39,094	39,566
	Higher	39,152	38,915	39,388
1425	Lower	37,828	37,592	38,064
	Higher	38,411	38,175	38,647

Standard Error = 80.84
All units for Means and Confidence Interval are psi.

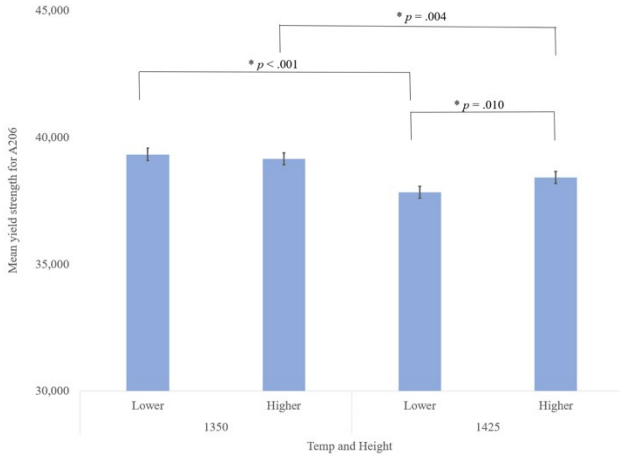

Figure 6. The LMM marginal means for yield strength A206 (and 95% confidence intervals) by temperature (temp) and pouring height (height).

To understand the interaction effect of A206 yield strength, a pouring temperature comparison within pouring height was performed. For lower pouring height, there was a significant difference in the mean yield strength for A206 between 1350F (732C) and 1425F (774C) (p < .001, mean difference = 1,501 psi (10.35 MPa) (, 95% CI of mean difference = 1,167 to 1,835 psi (-8.05 to 12.65 MPa). This was also the case for higher pouring height (p = .004, mean difference = 740 psi (5.10 MPa) (, 95% CI of mean difference = 406 to 1,074.11 psi (2.80 to 7.40 MPa)) where pouring temperature was identified as significant in A206 yield strength properties. A comparison using pouring height for A206 yield strength within pouring temperature was performed. For 1350F (732C), there was no significant difference in the mean yield strength for A206 between the lower and higher pouring height groups (p = .203, mean difference = 178 psi (1.23 MPa), 95% CI of mean difference = -156 to 512 psi (-1.08 to 3.53 MPa). On the other hand, for 1425F (774C) pouring temperature, there was a significant difference in the mean yield strength for A206 between the lower and higher pouring height groups (p = .010, mean difference = -583 psi (-4.02 MPa), 95% CI of mean difference = -916.73 to -249.02 (-6.32 to -1.72 MPa).

A356

The LMM analysis results for yield strength for A356. Determined there was no significant interaction between pouring temperature and height on yield strength (F(1,19.05)=1.86, p = .188). Furthermore, there was neither a significant temperature main effect (F(1,19.05)=0.13, p = .723) or significant pouring height main effect (F(1,19.05)=0.45, p = .511). For the LMM analysis, the BIC for AR(1) covariance structure was 988.53. The constant variance for the AR(1) covariance structure was estimated to be 813,474.82 (Wald Z = 5.32,

p < .001), and the ρ (the correlation between adjacent bars) was estimated to be 0.09 (Wald Z = 0.65, p = .515). Table 6 provides the marginal means for yield strength estimated from LMM by pouring temperature and pouring height for alloy A356, and Figure 7 provides the LMM marginal means for yield strength and the corresponding 95% confidence intervals by pouring temperature and pouring height. The difference between the lower bound and upper bound confidence interval was approximately 1,000 psi (6.89 MPa) for all experimental conditions presented in Table 4. Similar to A356 tensile strength, lower pouring height exhibited higher mean yield strength at lower pouring temperature and was the highest value for all temperatures and pouring height. For higher pouring temperature of 1425F (774C), higher pouring height displayed a slightly higher mean yield strength of approximately 170 psi (1.17 MPa) than the lower pouring height.

Table 6. Means and Confidence Intervals for Yield Strength of A356 by Temperature (Temp) and Pouring Height (Height)

			95% Confidence Interval	
Temp	Height	Mean (psi)	Lower Bound	Upper Bound
1350	Lower	29,131	28,611	29,651
	Higher	28,633	28,122	29,143
1425	Lower	28,709	28,198	29,219
	Higher	28,879	28,369	29,369

Standard Error = 249.82
All units for Means and Confidence Interval are psi.

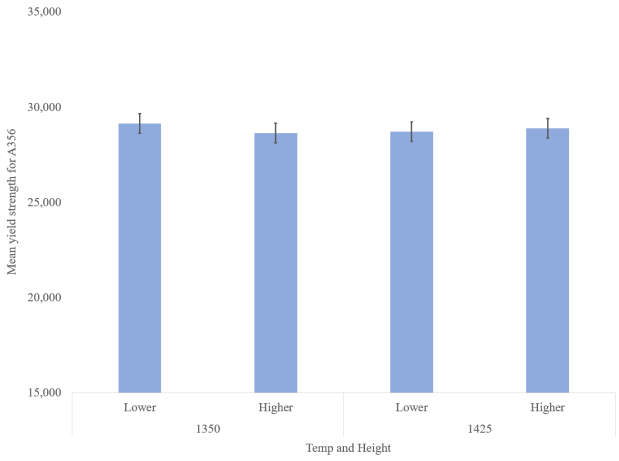

Figure 7. LMM marginal means for yield strength A356 (and 95% confidence intervals) by pouring temperature (temp) and pouring height (height).

LMM RESULTS FOR DUCTILITY

A206

Statistical analysis for A206 for ductility produced a BIC for AR(1) covariance structure equal to 288.72. The constant variance for the AR(1) covariance structure was estimated to be 6.24 (Wald Z = 4.42, p < .001), and the ρ (the correlation between adjacent bars) was estimated to be 0.37 (Wald Z = 2.49, p = .013). LMM results for A206 elongation indicated no significant interaction between temperature and pouring height ($F(1, 10.60) = 2.43$, $p = 0.148$). Main factor analysis showed there was neither a significant temperature effect ($F(1, 10.60) = 0.24$, $p = 0.637$) or significant height effect ($F(1, 10.60) = 0.68$, $p = 0.429$).

Table 7 provides the marginal means for elongation estimated from LMM by temperature and pouring height for alloy A206, and Figure 8 provides the LMM marginal means for elongation and the corresponding 95% confidence intervals by temperature and pouring height. Observation of the mean ductility shows highest elongation was achieved at low pouring temperature and height. For low pouring temperature, approximately 20% reduction in ductility occurred when the bars were cast at the higher pouring height. Tensile bars poured at higher temperature and both pouring heights exceeded the elongation properties of tensile bars produced at lower temperature and high pouring height by 11-17%. For higher pouring temperature, elongation properties were approximately 6% higher when the tensile bars were cast at a higher pouring height.

Table 7. Means and Confidence Intervals for Ductility of A206 by Temperature (Temp) and Pouring Height (Height)

			95% Confidence Interval	
Temp	Height	Mean	Lower Bound	Upper Bound
1350	Lower	10.89	9.00	12.79
	Higher	8.85	6.95	10.75
1425	Lower	9.97	8.08	11.87
	Higher	10.60	8.71	12.50

Standard Error = 0.86
All units for Means and Confidence Interval are percent.

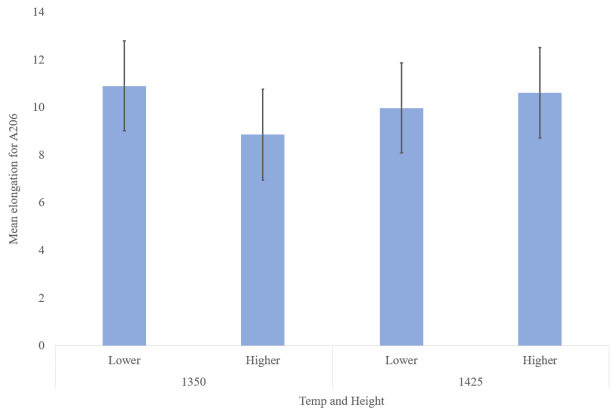

Figure 8. LMM marginal means for elongation A206 (and 95% confidence intervals) by pouring temperature (temp) and pouring height (height).

A356

For the statistical analysis, the BIC for AR(1) covariance structure was determined to be 116.03. The constant variance for the AR(1) covariance structure was estimated to be 0.29 (Wald Z = 5.48, p < .001), and the ρ (the correlation between adjacent bars) was estimated to be -.08 (Wald Z = -0.58, p = .560). LMM results showed there was no significant interaction between temperature and height on elongation properties for A356 ($F(1, 22.32) = 0.17$, $p = 0.683$). Analysis of the main factors indicated there was no significant pouring height effect ($F(1, 22.32) = 3.86$, $p = 0.062$) but, on the other hand, there was a significant temperature effect on elongation for A356 ($F(1, 22.32) = 21.79$, $p < 0.001$).

Table 8 provides the marginal means for elongation estimated from LMM by temp and height for alloy A356, and Figure 9 provides the LMM marginal means for ductility and the corresponding 95% confidence intervals by pouring temperature and height. The ductility properties were achieved at the lower pouring temperatures with the highest pouring height yielding a 4% improvement in elongation. Lower ductility properties, between 10-12% reduction, were observed at the higher pouring temperature. Similar to the lower pouring temperature, higher pouring height showed a 6% improvement in elongation properties.

Table 8. Means and Confidence Intervals for Ductility of A356 by Temperature (Temp) and Pouring Height (Height)

			95% Confidence Interval	
Temp	Height	Mean	Lower Bound	Upper Bound
1350	Lower	5.27	5.01	5.54
	Higher	5.47	5.21	5.73
1425	Lower	4.63	4.37	4.90
	Higher	4.93	4.67	5.20

Standard Error = 0.13
All units for Means and Confidence Interval are percent.

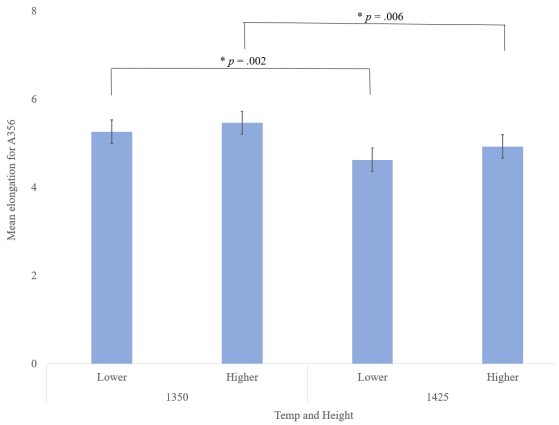

Figure 9. LMM marginal means for elongation A356 (and 95% confidence intervals) by pouring temperature (Temp) and pouring height (Height).

Given there was a significant temperature effect on elongation for A356 without a significant interaction between temperature and height on the outcome, a statistical evaluation was performed to determine the estimated means and standards errors from the LMM for elongation by temperature. A temperature of 1350F (732C) resulted in a higher mean elongation for A356 than a temperature of 1425F (774C) (mean = 5.37 vs. 4.78, respectively) by 0.59 units, on average ($p < 0.001$, 95% CI for difference in means = 0.33 to 0.85 units). Results for elongation at A356 by pouring height indicated no significant difference in the outcome between the two heights (mean = 4.95 for lower vs. 5.20 for higher, $p = 0.062$, 95% CI for difference in means = -0.51 to 0.01 units).

DISCUSSION OF RESULTS

The research work demonstrated that mechanical properties of aluminum alloys are influenced primarily by temperature, though the significance on properties varied between the investigated alloys. For tensile strength, there was no significant effect of the main factors of pouring temperature and height nor factor interaction between the

main factors for A206. For the case of A356, only an interaction effect between pouring temperature and height was determined. Interaction isolation of temperature indicated it was predominant only at low pouring height whereas higher pouring height was not influential.

No significant effects were determined for A356 yield strength for the main factor or interaction effect. A206 alloy showed statistical significance for the pouring temperature and the interaction effect between pouring temperature and height on yield strength. Detailed analysis of the interaction significance showed pouring height, either at low or high level, was influenced by pouring temperature. When the isolation analysis of pouring temperature was performed, the higher pouring temperature was only significant on pouring height, not low pouring temperature.

Ductility properties for A206 showed no significance on the main factors of pouring temperature, pouring height, and interactions between the main factors. The main factor of pouring temperature was shown to be significant for A356 ductility properties but pouring height factor and interaction were negligible on mechanical properties variation.

The scope of the research work considered the possible factors in pouring aluminum casting but was unclear on the direct cause to changes in mechanical properties. Clearly, temperature was a critical factor in mechanical properties and pouring height, in general, is not serious. However, practically all properties of both investigated aluminum alloys exhibited best properties for low pouring height occurring at low pouring temperature whereas at higher pouring height, best properties were obtained when poured at higher temperatures. It surmised that temperature, based on aluminum thermodynamic behavior, as shown in Figure 1, does not have a strong relationship in oxide influence on mechanical properties because oxides are less stable at higher temperatures. It may be plausible that temperature alters the oxide inclusion characteristics and air entrainment mechanism based on the pouring stream similar to Figure 2. This warrants research considerations in understanding the role of pouring temperature since pouring height has a minimal contribution as demonstrated in the statistical analysis.

Another interesting observation is the difference in how mechanical properties are influenced by pouring conditions between A206 and A356. Though there is no correlation shown in the present research that directly attributes oxide inclusions causing these mechanical properties changes, the role of solute additions does seem important. One possible hypothesis is the solidification microstructure developed by solutal additions. Figure 10 show typical microstructures of A356 and A206.[8] Clearly, A356 is approximately 50% eutectic phase with α-Al and Si between the dendrites whereas A206 has small amount of Al_2Cu eutectic phase between the dendrites. Though not investigated and assuming oxide inclusion formed during pouring was the cause of the changes in mechanical properties, location of the oxide inclusion would appear to have a critical role. If the oxide inclusion is assumed to reside at the dendrite boundary interface, both alloys should have some correlation to mechanical properties significance effects either as a main effect or interaction. The present research work does not exhibit this association and should be investigated further.

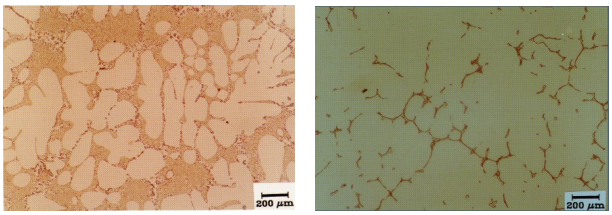

(a) *(b)*

Figure 10. Photomicrographs from "Solidification Characteristics of Aluminum Alloys Volume 3: Dendrite Coherency" (a) Microstructure of A356 and (b) Microstructure of A206.[8]

CONCLUSION

Statistical analysis of the experiment indicates pouring temperature is a predominant factor, either as a main factor and part of an interaction effect, on the properties of aluminum alloys. A356 showed a significance, either as a main effect or interaction effect, only for tensile strength and ductility. On the other hand, A206 only showed an influential effect on yield strength.

Pouring height, as a main factor, showed no significance on mechanical properties of A206 or A356. Low pouring temperature at low pouring height produced the best mechanical properties for both alloys whereas at high pouring temperature, higher pouring height generated better mechanical properties. Though unclear of this behavior for both alloys, an oxide film on the pouring appears to provide some beneficial effect irrespective of the pouring height and chemistry.

Interestingly, if one alloy showed a significant influence of a mechanical property, the other alloy did not exhibit any significance. One possible hypothesis on the alloy property variances was microstructural differences between A206 and A356. Another possible cause is the role of temperature in altering the fluid dynamics characteristics that produce low volume air entrainment or dispersion behavior differences. Both of these hypotheses are recommended for future investigations to advance

research initiatives in machine learning and digital twin development.

ACKNOWLEDGMENTS

Research work was sponsored by the DLA Troop Support, Philadelphia, PA, and the Defense Logistics Agency Information Operations, J68, Research & Development, Ft. Belvoir, VA under contract numbers SP4701-18-D-1200 and SP4701-18-F-0070, titled "Investigation of Dross Mechanism for Highly Oxidative Casting Alloys." The authors would like to acknowledge Carley Foundry for participating in the research work and greatly appreciate the effort of everyone involved who assisted in the pouring and processing of the castings.

REFERENCES

1. Majidi, S.H. and Beckermann, C. "Effect of Pouring Conditions and Gating System Design on Air Entrainment During Mold Filling," *International Journal of Metalcasting*, Volume 13, Issue 2 (2019).
2. Majidi, S.H. and Beckermann, C., "Modelling of Air Entrainment During Pouring of Metal Castings," *International Journal of Cast Metals Research*, 30:5, 301-315 (2017). doi: 10.1080/13640461.2017.1307624 (Link last accessed 02-12-25.)
3. Reilly, C., Green, N.R., Jolly, M.R., and Gebelin, J.C., "The Modelling of Oxide Film Entrainment in Casting Systems Using Computational Modelling," *Applied Mathematical Modelling*, 37 (2013), 8451-8466.
4. Relph, S. and Kiger, K.T., "Air Entrainment and Subharmonic Waves Induced by a Forced Plunging Jet," *Experiments in Fluids* (2021).
5. "Ellingham Diagrams," University of Cambridge, https://www.doitpoms.ac.uk/tlplib/ellingham_diagrams/printall.php (Link last accessed 02-12-25.)
6. Runyoro, J., Boutorati, S.M.A., and Campbell, J. "Critical Gate Velocities for Film Forming Casting Alloy: A Basis for Process Specification," *AFS Transactions*, Volume 37, pp 225-34 (1992).
7. "IBM SPSS Advanced Statistics 28," IBM Corp, 2021; p. 79-83 (Link last accessed 02-12-25.)
8. Arnberg, L., Bäckerud, L., Chai, G., "Solidification Characteristics of Aluminum Alloys, Volume 3: Dendrite Coherency," American Foundry Society, pp. 78 and 103 (1996).